Convergence
A Journal for Young Researchers

ORIGINAL RESEARCH

Received: 2-25-26; Accepted: 6-3-26;
Managing Editor: Jonas Katona;
Action Editor: Feiyuan Long

A Magnetostatic Analysis of Magnetic Saturation's Impact on PMSM Overall Efficiency and Copper Losses Under Varying Load Conditions

Guilherme Yuji Oliveira Kikuchi

Colégio Miguel de Cervantes, São Paulo, Brazil

Abstract

Currently, electric motors have a wide range of applications across industries and they are one of the pillars in the world's decarbonization, most notably the permanent magnet synchronous motor (PMSM) due to its efficiency compared to others. This paper's purpose is to analyze the impact of operating a saturated PMSM, under load condition variations, on overall efficiency and copper losses using a finite element analysis (FEA), for which a two-dimensional finite element model was developed in Ansys Maxwell Student software. RMS current was increased in order to simulate load variations; then, electrical power input and mechanical power output were both measured in watts and evaluated to analyze efficiency degradation and copper losses on saturated conditions. The simulation results show that the increasing current supplied to a saturated system does not proportionally equate to magnetic flux density gains, plateauing after increasing beyond the range of values saturation starts, stalling electromagnetic torque, as a result the mechanical power output stagnated. Conversely, as the electrical power input continued to rise it was dissipated as heat rather than mechanical output, hence reducing the overall efficiency. Therefore, the results met the hypothesis, which established that more current driven into the PMSM would not proportionally increase magnetic flux density, gains in mechanical power output would diminish to the point it stagnates, and excess current piles on copper losses, thence reducing overall efficiency. This paper can be used to further understand the effects of magnetic saturation on a PMSM's overall efficiency and copper losses to optimize electrical power usage.

Keywords: permanent magnet synchronous motor (PMSM), magnetic saturation, finite element analysis (FEA), copper losses, efficiency degradation, torque-current nonlinearity, B-H curve, magnetostatic modeling, load variation via current sweep

1. Introduction

In the modern day, electric motors are used in a variety of utilities that range from basic household appliances to heavy industrial machinery (Saidur, 2010). In fact, they are one of the fundamental pillars in the context of global decarbonization, since electric motors generate lower greenhouse gas (GHG) emissions in comparison to internal combustion engines (ICEs) during their use phase (Tagliaferri et al., 2016). However, this is subject to fluctuations among countries due to the differences in the energy source used for power generation. Moreover, a comparative analysis on the overall efficiency between electric vehicles (EVs) and internal combustion engine vehicles (ICEVs) concluded that the efficiency from battery to wheels ranges from 50% to 80%, whereas the most efficient ICEVs reach efficiencies of 42% from tank to wheels. Nonetheless, it is necessary to consider the energy source used and its efficiency to generate the electricity to provide a more well-rounded analysis, namely, well-to-wheel. In this perspective, EVs' efficiency can drop to similar or lower levels than those found in ICEVs (Albatayneh et al., 2020).

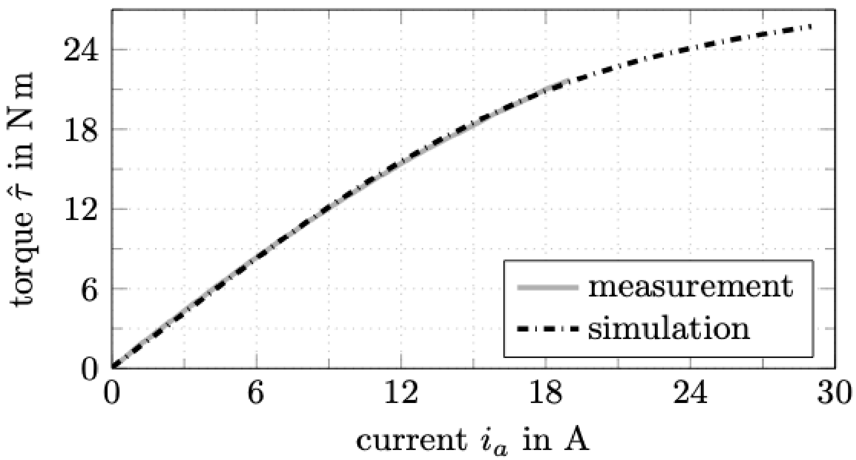

Figure 1: Relationship between torque and electric current (Faustner et al., 2015).

Note: The graph shows torque versus current of a simulated PMSM, showing a nonlinear behavior at higher current levels.

Despite the fact that electric motors are more efficient overall, they have a fundamental restraint: magnetic saturation. Magnetic saturation is produced when the magnetic field strength (H) continues to increase, but the magnetic flux density (B) does not increase at the same rate, achieving a plateau (Pjevalica et al., 2015). This circumstance arises in response to higher mechanical loads being applied to the motor, requiring more current to strengthen the magnetic field within the core. Nevertheless, the addition of more current into the system, beyond a certain range of values, drives the core into saturation. For that reason, any further increases in current do not provoke an equivalent gain in magnetic flux density, limiting torque production, thus capping the mechanical power output (See Figure 1). Additionally, providing additional current into a saturated motor produces a disproportionate gain in mechanical power output, causing a large amount of the excess electrical power input to be dissipated as heat, accounting for 55-60% of all losses in efficiency. Specifically, they are called I2R losses, since they are derived after Joule's law; hence, as more current is driven into the system, the thermal losses increase as well (Saidur, 2010).

Previous work on magnetic saturation indicates that the primary cause of magnetic saturation is higher load conditions, which lead to an increase in current supplied to the stator windings. As a consequence, the magnetic field strength (H) increases, but the stator's magnetic flux density (B) does not increase as much due to size and material strains.

Other studies that analyzed the consequences of saturation on the mechanical power output found a nonlinear relationship between current and torque production. Even though torque keeps increasing with a greater current, the rate at which torque grows reduces significantly under saturation situations, signaling that any excess electrical input does not relate proportionally to the motor's mechanical output (Chen et al., 2016; Liu et al., 2018; Faustner et al., 2015).

Similarly, research on PMSMs frequently states that higher current increases copper losses. These losses reduce energy conversion efficiency (Burt et al., 2008; Li et al., 2025; Liu et al., 2018; Atay, 2000).

The combination of the existing literature establishes that the operation of motors in overload leads to saturation, providing higher electrical power input, which increases disproportionately relative to the mechanical power output and escalates the percentage of power lost due to heating. However, there is a gap in the present work, which mainly focuses on each of these effects separately and lacks an explicit graphical representation of the power converted into heat and mechanical output when the system is already saturated. Also, researchers do not agree on a common behavior that efficiency suffers as the load varies when the motor is subjected to saturation conditions.

This paper intends to establish a relationship between load variations on a PMSM operating under saturation conditions and the energy converted into mechanical output and copper losses. It is expected that a PMSM, in saturation, with increasing load conditions, causes the PMSM to draw additional current into the system, but the corresponding mechanical output experiences increasingly smaller gains; this disproportion between electrical power input and mechanical power output reduces the motor's overall efficiency. However, this has not been properly connected within the existing literature; in this sense, the purpose of this paper is to establish the relationship between those motor properties affected by magnetic saturation by conducting a PMSM's magnetostatic simulation and building upon the literature. This paper is organized as follows: section 2 expands the theoretical background with more context of magnetic saturation effects and the PMSM structure; in section 3, the methods and the PMSM's specific configuration are described; section 4 presents and analyzes the results of the 2D simulation on the impact of operating a saturated PMSM on its properties; section 5 discusses the significance of the results, limitations, and a comparison to the literature reviewed to guide the simulation and paper; and finally, section 6 concludes the paper with some suggestions on future research.

2. Context

2.1. Mechanical output in saturation

As aforementioned in the literature review, magnetic saturation happens when the magnetic field strength (H), measured in amperes per meter, continues to increase, but the magnetic flux density (B), measured in Tesla, does not increase proportionally.

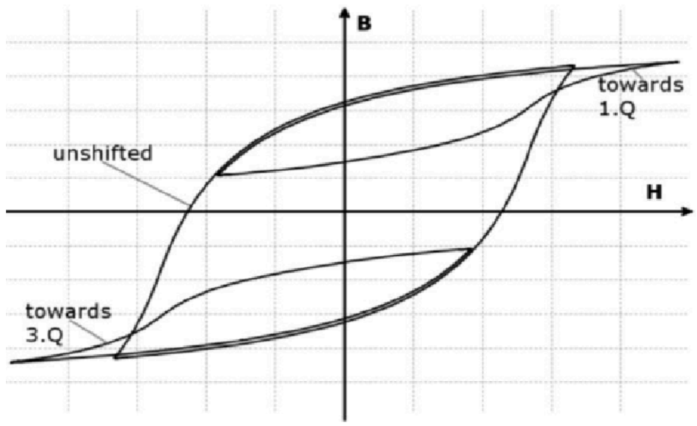

Figure 2: B-H behavior of the stator core by the influence of the windings' induced magnetic field (Pjevalica et al., 2015).

Note: This figure exhibits the B-H curve that follows a nonlinear behavior as the magnetic field strength increases due to higher current levels.

This behavior can be further understood when the equation that links B and H is analyzed:

$$B = \mu_0 (H + M(H)) \qquad (1)$$

Where $\mu_0 = 4\pi\, 10^{-7}\, [T\, m\, A^{-1}]$ is the constant of vacuum's magnetic permeability, and M is the material magnetization, measured in A/m. At first, magnetization increases in proportion to H, but the material has a magnetization limit, causing M to plateau despite increases in H.

In this sense, the range of values in which saturation starts can be identified based on the reduction of the incremental slope. This method consists of comparing in a ratio the local slope of certain values in low current and at higher current, setting a measurable bar to compare increases, in which 1 means they are the same, and they become smaller as saturation is achieved (Zhu et al., 2021).

The direct relationship between torque and magnetic flux density explains the reason why the stagnation in magnetic flux density limits torque production. The formula used to calculate torque, in most 2D FEA models, is based on the Maxwell stress tensor surface integral that calculates the electromagnetic torque (T_e). The equation is displayed below: (Popescu, 2006; Shin et al., 2021)

$$T_e = \frac{1}{\mu_0} \int_0^{2\pi} r^2 B_r B_\theta \, d\theta \quad (2)$$

Where B_r B_θ are the radial and tangential components of the flux density B, r is the radius of the circle limited by the outer diameter of the air gap. In 2D models, the surface integral from the Maxwell stress tensor is turned into a line integral along the air gap.

Likewise, when torque stagnates, the mechanical power output is also stalled, because it is proportional to the torque, as it is shown in the equation below:

$$P_{mech} = T_e \times \omega \qquad (3)$$

Where P_{mech} is the mechanical power output, T_e is the electromagnetic torque used in FEA simulations, and ω is the PMSM's angular speed, measured in RPM. In most PMSM simulations, angular speed is assumed to be constant, since magnetic saturation does not directly relate to the angular speed formula. Additionally, the only situation that could impact the angular speed is in the case that the load exceeds the saturated torque capability, meaning that the motor cannot sustain a constant angular speed, as a result decreasing the angular speed.

2.2. Overall efficiency

A motor's overall efficiency is calculated based on the ratio between mechanical power output and electrical power input, illustrated in the formula below:

$$\eta = \frac{P_{mech}}{P_{elec}} \qquad (4)$$

While electrical input soars, mechanical power output does not increase by the same amount when the motor is saturated, reducing overall efficiency. Furthermore, if overall efficiency drops, the excess energy needs to be converted into another sort of energy: thermal energy that is possible to predict using Joule's law:

$$P = n\, I^2 R(T) \qquad (5)$$

Where the resistance (R) is dependent on the coil's temperature (T) and n is the number of motor phases. Since the formula depends on current, it is expected that losses will mount as more current is driven into the system. (Tong et al., 2025)

However, it is important to acknowledge that there are more types of losses: iron, friction, windage, and stray losses. Iron, friction, and windage losses are considered independent of the load, meaning that more current will not increase these types of losses; also, they make up around 26% of losses, which is small compared to almost 60% that copper losses achieve as the load is increased. Although the stray losses are generally proportional to the square of the current in the stator, they only comprise 15% of all losses. In this sense, copper losses were only taken into consideration due to their significance compared to the other losses and their relationship with electric current.

2.3. Permanent Magnet Synchronous Motor (PMSM)

A PMSM is a type of AC electric motor that consists of two main parts: the stator and the rotor (see Figure 3). The stator consists of two components: the stator core and the stator windings. The core is composed of laminated silicon sheets to house the stator windings and reduce energy loss; the stator windings are sets of coils wound inside cages within the stator's core and are fed with electric current to create a rotating magnetic field. Similarly, the rotor has two components: the rotor core and permanent magnets. The rotor core serves almost the same utility as the stator core; it is the structure that sustains the permanent magnets that will rotate due to the induced rotating magnetic field. In this case, the rotor core was a surface-mounted rotor; the permanent magnets supply a constant magnetic field that will make the rotor rotate when interacting with the stator's windings. In addition, like any other AC motor, PMSMs have phases. To most closely emulate a real PMSM, it was chosen to use the most common number of phases: three (Mersha & Du, 2022).

3. Methods

In this section, a complete description of the PMSM configuration is shown based on the details of the numerical model imported and modified. Additionally, the methodology used to investigate the effects of operating a saturated PMSM on its overall efficiency and copper losses is presented.

3.1. Configuration

The surface-mounted PMSM model was imported from RMxprt's examples file, a tool embedded in the Ansys Maxwell student version software. Tables 1, 2, and 3 show the motor's structural parameters, and Figure 3 shows a picture of the motor's design (Mersha & Du, 2022).

Table 1: Stator's specifications.

Parameters	Values
Stator outer diameter	120 mm
Stator inner diameter	75 mm
Length of stator core	65 mm
Stacking factor	0.95
Steel type	M19-24G
Number of slots	24

Slot type	2
Skew width	0

Table 2: Rotor's specifications.

Parameters	**Values**
Rotor outer diameter	74 mm
Rotor inner diameter	26 mm
Length of the rotor core	65 mm
Steel type	M19-24G
Stacking factor of rotor core	0.95
Number of poles	4
Pole type	1
Air gap	1 mm

Table 3: Permanent magnet's specifications

Parameters	**Value**
Embrace	0.7

Offset	0 mm
Magnet type	Ceramic8D
Magnet thickness	3.5 mm

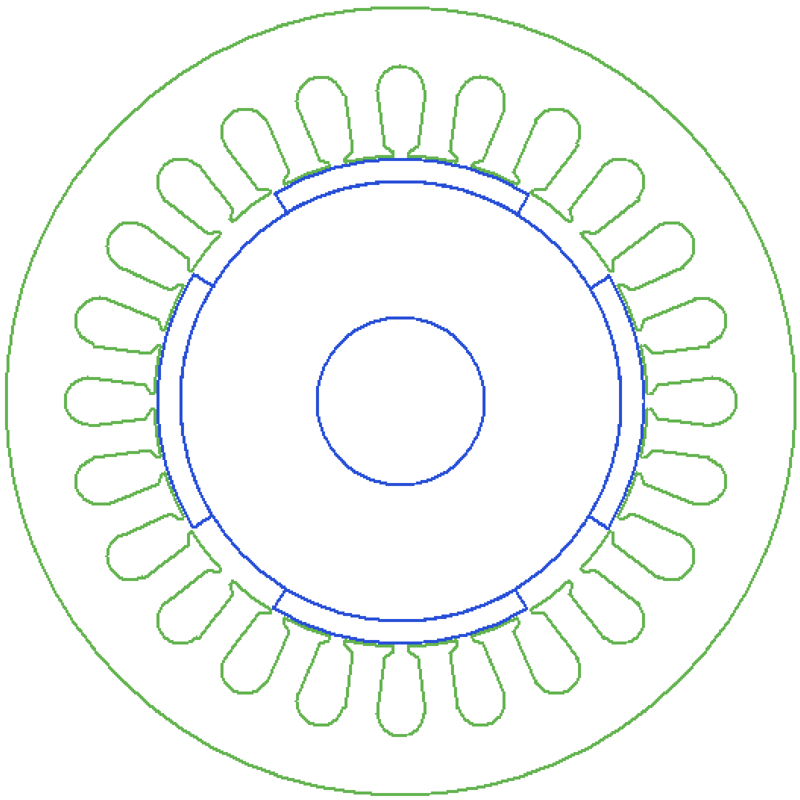

Figure 3: RMxprt modified model.

Note: The cross-sectional view of the 2-D PMSM model setup, with the stator and rotor highlighted in green and blue, respectively. Image obtained from the researcher's experimental setup in Ansys Maxwell.

A two-dimensional model was chosen, since the differences with a three-dimensional model are minimal, and a 2-D model demands less computational capacity in order to simulate the parameters.

3.2. Numerical model

The solution type used for the simulation was magnetostatic. Moreover, the constant variables were the angular speed fixed at 2000 rpm to represent steady state, and the resistance was fixed at a temperature of 75°C. There were two different parametric sweeps: root mean square (RMS) current and mechanical angle. RMS current was the variable modified to emulate load variations, using the parametric sweep tool. Nonetheless, it is important to consider that even though mechanical load and RMS current are related, it is a simplification of a far more complex relationship involving only the q-axis current component of the RMS current. Nevertheless, at normal operating conditions, the d-axis component is approximately 0, meaning RMS current is similar to the q-axis magnitude (Gundogan & Bakan, 2026). In addition, its parametric sweep was introduced to find at which range of current values saturation occurs by comparing different increases experienced in magnetic flux density at distinct current values. Secondly, the electric current was increased beyond the range at which saturation begins, and evaluated by how it influences mechanical power output. Then, the mechanical angle sweep was made at some punctual electric current values to find the average torque output as the current increases. Afterwards, using the result found for average torque, the mechanical power output was calculated by plugging the values into the mechanical power formula. Subsequently, overall efficiency was calculated using the ratio between mechanical power output at specific current values and electrical power input, which was estimated by adding copper losses and mechanical output, since copper losses account for more than half of total losses in electric motors (Saidur, 2010).

4. Results

Although magnetic flux density continues to increase, it follows a nonlinear path that reduces the pace at which B increases as the current becomes greater. For instance, to increase one T in flux density, initially, it takes about a 15 A increase, but the next increase of one T demands 63 more A than the last increase. That means that the magnetic flux density produced by the current starts to stabilize, since it takes more than four times the current to increase it by the same amount.

Moreover, the incremental slope between the increase experienced from 1 to 15 A, where most prominent gains seem to be concentrated, is approximately 0.55 T, whereas the increase experienced from 16 to 30 A, the next 15 A of current, is nearly 0.27 T. The ratio between those two slopes is 0.49, which means that although only 15 A apart, the second slope is already 49% of the first, showing that saturation possibly starts within 10 to 20, where increases get significantly smaller. Conversely, if comparing the increases from 16-30 A and 31-45 A, the ratio becomes 0.82, indicating magnetic flux density is stabilizing. Consequently, increasing current input saturates the magnetic flux density, which in turn limits torque production.

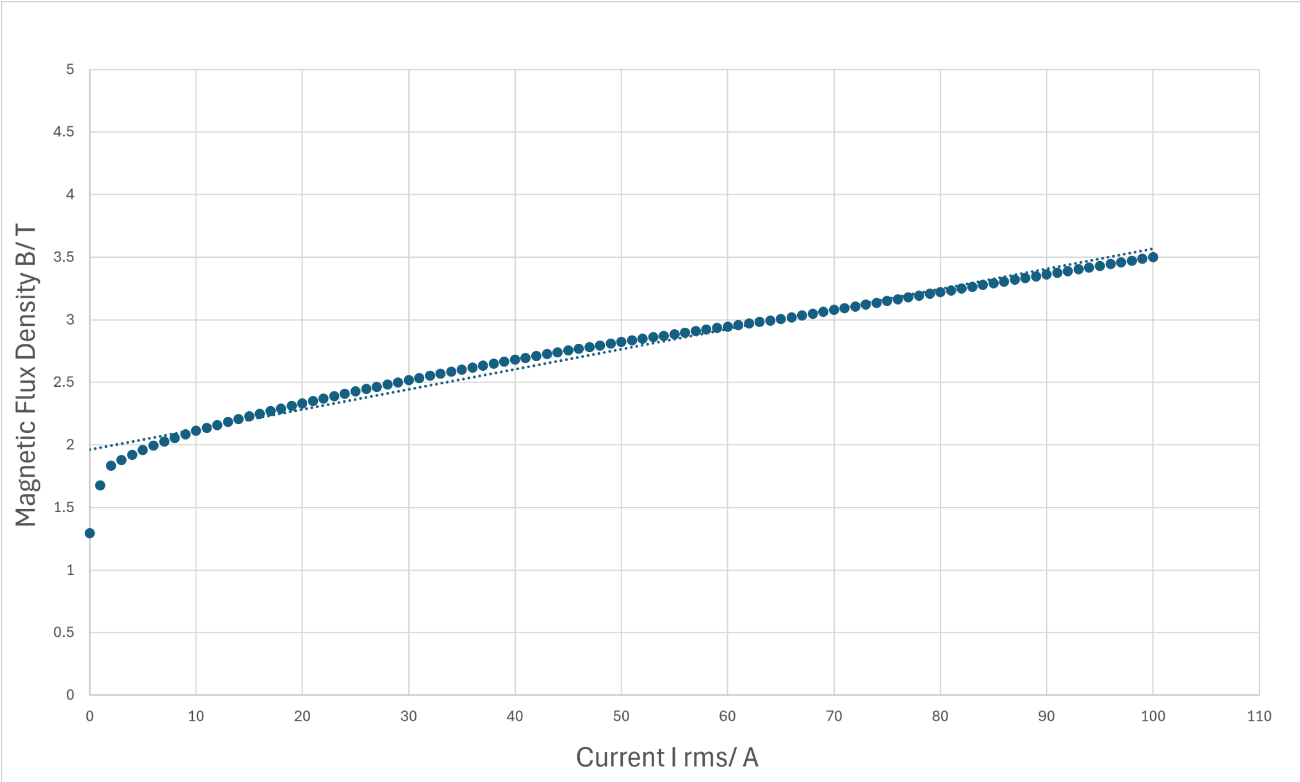

Figure 4: Magnetic flux density vs. I RMS graph, generated in Microsoft Excel with a linear regression fit overlaid.

Note: The graph shows the relationship between RMS current and the maximum magnetic flux within the stator. Each point corresponds to a value of magnetic flux density for currents from zero to 100 A.

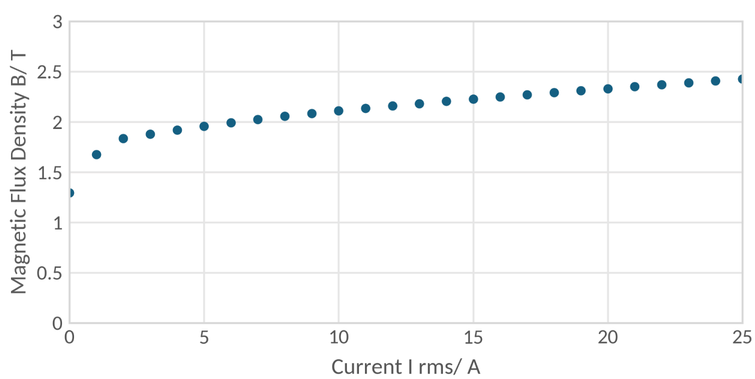

Figure 5: Magnified view of the Magnetic flux density vs. I RMS graph, generated in Microsoft Excel.

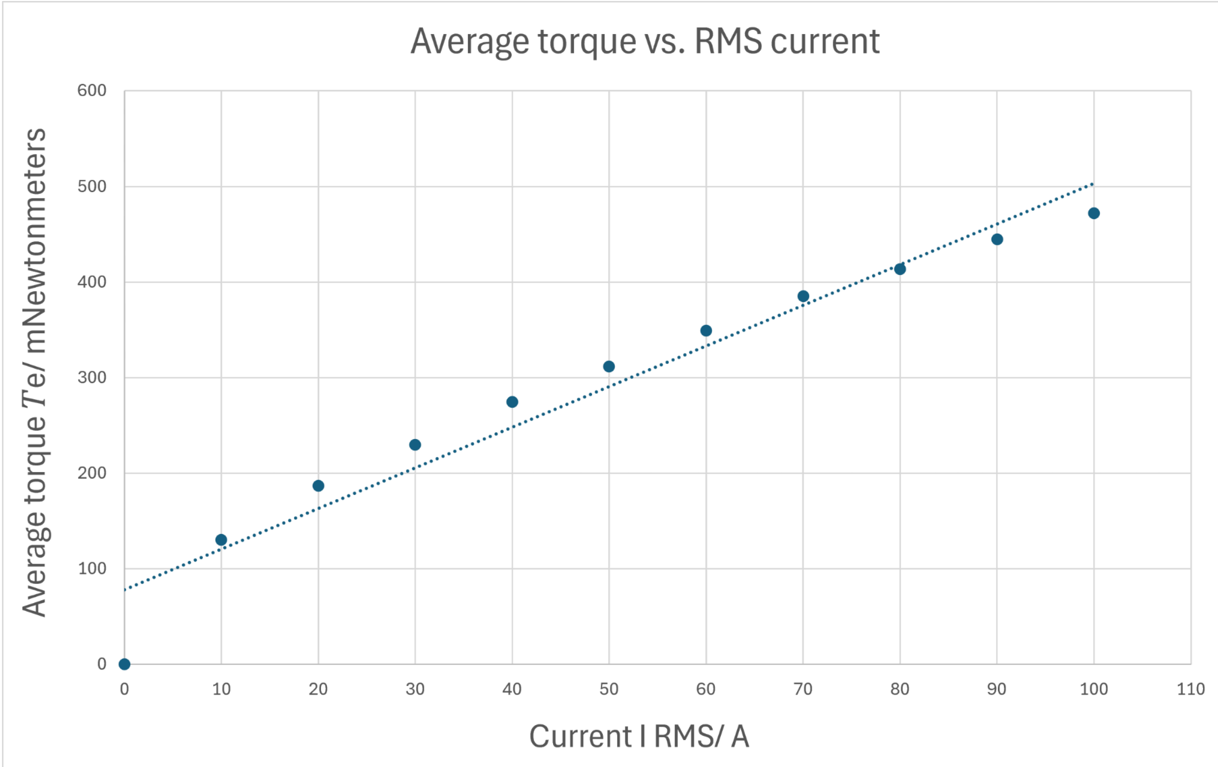

Figure 6: Average torque vs. RMS current graph, generated in Microsoft Excel with a linear regression fit overlaid.

Note: This graph presents the variation of average torque with increasing current. Average torque values are binned by 10 A of current input. The trend followed by the average torque is nonlinear, almost logarithmic.

Figure 6 showcases signs that the average torque started to stabilize after a sequence of increases in current, reducing the rate of gain in torque. For example, the increase produced by the first 10 A is 130 mNewtonmeters, whereas the increase of 10 A from 90 A to 100 A is 27 mNewtonmeters, showing a reduction of 79.3% in the ratio of increments in average torque, aligning with the disproportionality shown previously for magnetic flux density, since it caps torque production. Since torque is one of the components of mechanical power, its stabilization stalls mechanical power values.

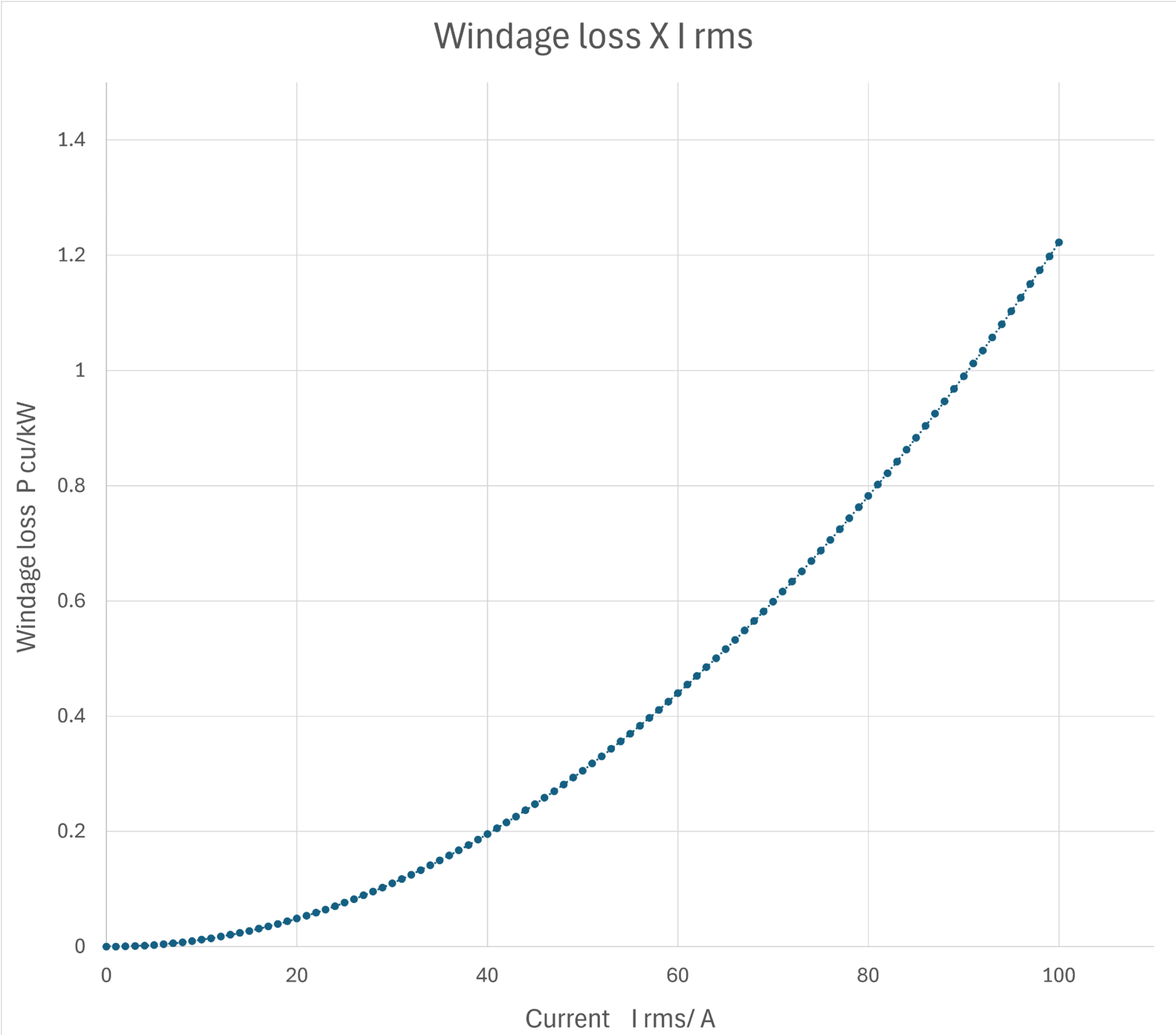

Figure 7: Copper losses vs. I RMS graph, generated in Microsoft Excel with a quadratic fit overlaid.

Note: The graph of Figure 7 illustrates copper losses as a function of RMS current; each value of power lost due to heat is spaced by 1 A from 0 to 100 A, exhibiting a behavior close to exponential growth.

The behavior illustrated in this figure is close to exponential growth, since the rate of copper loss increases steeply at every step, exemplified in the final values as the separation among the points becomes more prominent. Up to 40 A, copper losses comprise approximately 200 watts, but as current increases to 60 A, losses are more than twice the value registered at 40, and at 100 A, copper losses are responsible for more than 1,200 watts. This scenario is one where the PMSM increases electrical power input, trying to make up for increasing load conditions, but this behavior causes magnetic saturation and compounds copper losses. Therefore, as shown in Fig. 6, operating a PMSM beyond the start of saturation can massively impact the amount of electrical power dissipated as heating, highlighting its impact on efficiency.

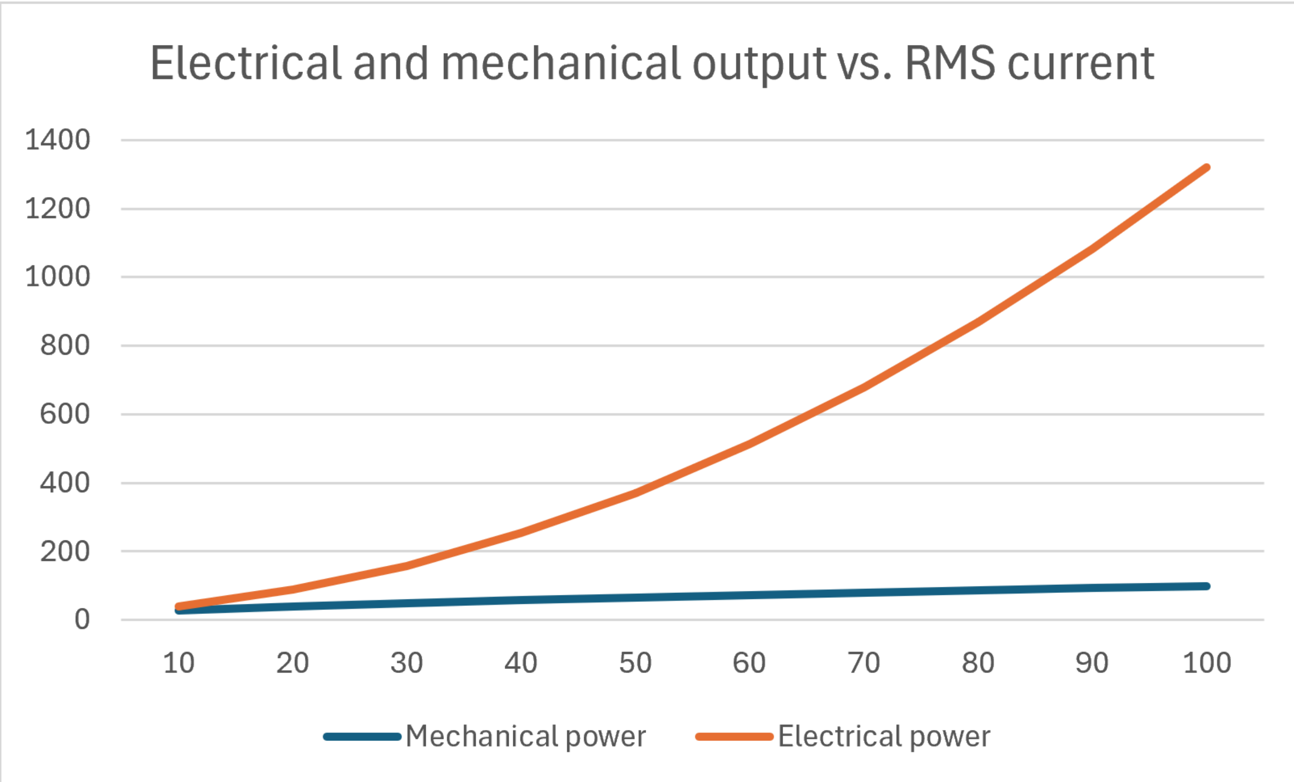

Figure 8: Electrical input and mechanical output vs. RMS current graph. Generated in Microsoft Excel.

Note: Figure 8 portrays a comparison between electrical power input, represented by the orange line, and mechanical power output, represented by the blue line, both as a function of RMS current. It highlights how mechanical output is outgrown by electrical input when factoring in saturation.

Electrical input was calculated by adding windage losses to the mechanical power output. Despite that, electrical input is underestimated, since iron core and eddy current losses were not taken into consideration (Saidur, 2010). Furthermore, for the mechanical output, due to the software's limitations and angular speed not being directly related to magnetic field density, the value of angular speed was chosen as 2000 rpm, which, converted into rad/s, is approximately 209. Nonetheless, the angular speed is fixed since it is a magnetostatic analysis.

In lower electrical power input values, the mechanical output is almost equivalent to it, but as the current increases beyond where saturation starts, the mechanical output starts to stall. The electrical power input skyrockets, whereas the mechanical power output does not follow up; it stabilizes and achieves a plateau at 98 watts. This difference between electrical power input and mechanical power output is staggering to the point that it is more than 1,119 watts. The stagnation of torque and the steep increase of copper losses cause such disparity between them, making it reasonable to understand why overall efficiency drops when operating a PMSM in saturation.

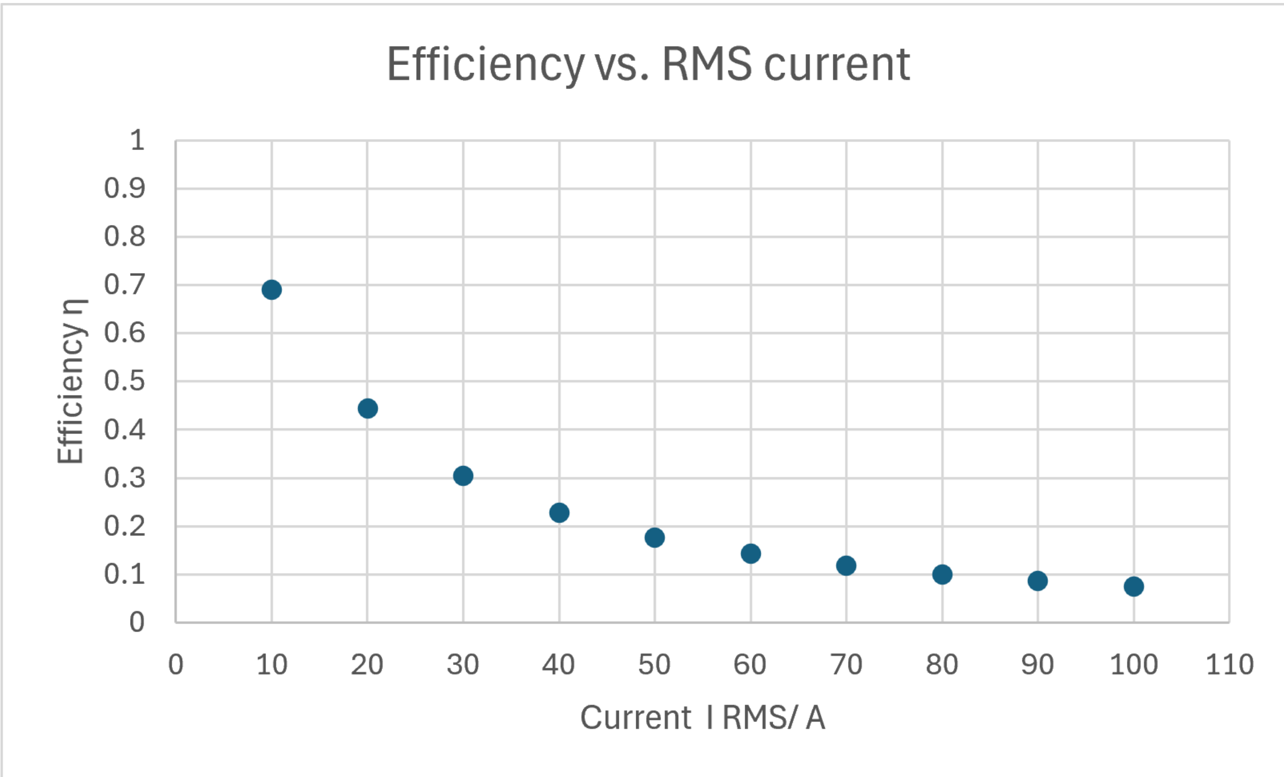

Figure 9: Efficiency vs. RMS current graph, generated in Microsoft Excel.

Note: Figure 9 is a scatterplot of the RMS current and the overall efficiency calculated at 10 A. This scatterplot presents the decline in efficiency as a consequence of the previous results.

This scatterplot exposes how efficiency plummets as more current runs into the system, and it starts to converge towards 0, despite it not being possible unless the motor is stopped. At 10 A, efficiency is decently high at approximately 70%, but after surpassing 20 A, the efficiency is below 50 %, which continues to decline at a fast pace, reaching only at 7.47% efficiency when the current reaches 100 A.

5. Discussion

As stated in the hypothesis, it was expected that when load conditions are increased, the saturated PMSM would draw additional current into the system. However, the additional current would not be directly converted into mechanical output gains, but rather diminish gains as current increases. This nonlinear relation between electrical power input and mechanical power output was a result of the rapid increase in copper losses, causing overall efficiency to drop.

In this sense, as shown in the analysis, this behavior is followed. Figure 4 shows that more current does not equal proportional gains in magnetic flux density. Next, since the rate of gains in magnetic flux density was held back around 10-20 A, the average torque follows the same path. Since torque is affected, mechanical power growth was also impacted negatively, whereas copper losses rose sharply. Consequently, the disproportion between electrical power input and mechanical power output grows massively to the point that overall efficiency plummets, falling from around 70% at 10A to 7.5% at 100 A.

Nonetheless, this simulation and analysis have some limitations. In spite of using Ansys Student Maxwell for free, and it being one of the most detailed and widely used software, it brought some limitations. In the first place, a magnetostatic simulation was done, which is not the most realistic, since it assumes the motor is fixed at a given position and it does not move from that point, meaning that to have the average torque, a mechanical angle sweep was needed, and there was no angular speed output to have a more realistic simulation. Secondly, in magnetostatic simulations, it was not possible to change the load; the whole analysis was done with respect to electrical current, since it is directly related to load condition increases (Liu et al., 2018). In terms of losses, due to software limitations, temperature was fixed, in turn meaning resistance remains invariable, which results in an underestimation of losses even further, since that is not a realistic situation. Finally, efficiency was calculated by estimating electrical input as mechanical output plus copper losses, overestimating efficiency, since the other types of losses were neglected.

In comparison to previous research, this work connects the impact of increasing loads in causing magnetic saturation and the result of magnetic saturation on torque, efficiency, and thermal losses, which was the gap found in the literature. However, some of the papers reviewed had different materials, purposes, specifications, and approaches, meaning results may differ between different studies. Furthermore, this work only comprises PMSMs, meaning the results cannot be generalized to other motor types. Nonetheless, the results are consistent to prior work: the nonlinear behavior of the B-H curve, the relationship between increasingly higher electric current and torque (Faustner et al., 2015), the disproportion between increases in electric power input relative to mechanical power output (Chen et al., 2016; Liu et al., 2018; Faustner et al., 2015), fast rise of copper losses (Burt et al., 2008; Li et al., 2025; Liu et al., 2018; Atay, 2000), and the decline in overall efficiency.

This research is of extreme relevance in the current world scenario, as the world's decarbonization efforts rely heavily on EVs and clean energy production. Therefore, understanding the behavior of magnetic saturation and its implications on the electrical power efficiency of PMSMs can aid manufacturers in designing their motors to maximize efficiency and minimize losses, especially copper losses. Reducing these losses means that EVs can avoid unnecessary power consumption and diminish the number of recharges. Hence, the reduction in energy demand decreases the need for additional power generation and reduces GHG emissions of EVs, depending on the energy source used for electricity generation (Tagliaferri et al., 2016).

On the other hand, copper losses damage central pieces of PMSMs, implying more material is used to replace the damaged pieces. When temperature increases within the windings, copper heats up, and the excessive heat damages its insulation, leading to short circuits that interrupt the motors' functioning (Tong et al., 2025). Moreover, permanent magnets can be demagnetized permanently if their temperature surpasses a certain level, causing inevitable losses of rare-earth magnets (Guo et al., 2020). Therefore, copper losses can make PMSMs more harmful than beneficial to the environment, as those damages demand the extraction of more minerals, which is a highly polluting industry (Moghimi Dehkordi et al., 2024).

6. Conclusion

In this paper, the causes and consequences of magnetic saturation in an electric motor were discussed. A two-dimensional FEA simulation was set to further understand the impacts of magnetic saturation on a PMSM's efficiency and copper losses. The results confirmed that more current causes the magnetic flux density to stall, which is the primary sign of saturation. Then, it was demonstrated that the mechanical power output is flattened by the limited torque production. In contrast, electrical power input escalates at a faster rate than mechanical output due to the dramatic increase in copper losses, causing a sharp decline in overall efficiency.

This work was applied to a PMSM motor, though one of the most widely used, there are many different types of electric motors built with different materials and arrangements. Furthermore, size is a factor that can affect the range of values at which saturation starts in different motors. Other possible variations include more realistic resistance behavior and rpm.

Future work should focus on redoing the experiment following different approaches: three-dimensional FEA transient simulation, physical experimentation, and a combination with MATLAB and Simulink. A three-dimensional transient simulation provides a better insight into the real dynamics of a PMSM, since the simulation takes into consideration the motor's functioning over time and comprises a complete version of the motor. In comparison, a physical experiment is the most realistic way to understand the impacts of magnetic saturation. Finally, software like MATLAB and Simulink can be combined with the FEA simulation for a more complete analysis of the circuit.

7. References

Albatayneh, A., Assaf, M. N., Alterman, D., & Jaradat, M. (2020). Comparison of the Overall Energy Efficiency for Internal Combustion Engine Vehicles and Electric Vehicles. *Environmental and Climate Technologies*, 24(1), 669–680. https://doi.org/10.2478/rtuect-2020-0041

Burt, C. M., Piao, X., Gaudi, F., Busch, B., & Taufik, N. F. (2008). Electric Motor Efficiency under Variable Frequencies and Loads. *Journal of Irrigation and Drainage Engineering*, 134(2), 129–136. https://digitalcommons.calpoly.edu/eeng_fac/178/

Chen, X., Hu, J., Chen, K., & Peng, Z. (2016). Modeling of electromagnetic torque considering saturation and magnetic field harmonics in permanent magnet synchronous motor for HEV. *Simulation Modelling Practice and Theory*, 66, 212–225. https://doi.org/10.1016/j.simpat.2016.02.012

Faustner, D., Kemmetmüller, W., & Kugi, A. (2015). Magnetic Equivalent Circuit Modeling of a Saturated Surface-Mounted Permanent Magnet Synchronous Machine. *IFAC-PapersOnLine*, 48(1), 360–365. https://doi.org/10.1016/j.ifacol.2015.05.033

Gundogan, A., & Bakan, A. F. (2026). Torque Ripple Reduction in Surface-Mounted Permanent Magnet Machine with Model-Based Current Reference Control. *Electronics*, 15(6), 1240. https://doi.org/10.3390/electronics15061240

Guo, H., Ding, Q., Song, Y., Tang, H., Wang, L., & Zhao, J. (2020). Predicting Temperature of Permanent Magnet Synchronous Motor Based on Deep Neural Network. *Energies*, 13(18), 4782. https://doi.org/10.3390/en13184782

Liu, Y.-X., Li, L.-Y., Cao, J.-W., Gao, Q.-H., Sun, Z.-Y., & Zhang, J.-P. (2018). The Optimization Design of Short-Term High-Overload Permanent Magnet Motors Considering the Nonlinear Saturation. *Energies*, 11(12), 3272. https://doi.org/10.3390/en11123272

Mersha, T. K., & Du, C. (2022). Co-Simulation and Modeling of PMSM Based on Ansys Software and Simulink for EVs. *World Electric Vehicle Journal*, 13(1), 4. https://doi.org/10.3390/wevj13010004

Moghimi Dehkordi, M., Pournuroz Nodeh, Z., Soleimani Dehkordi, K., Salmanvandi, H., Rasouli Khorjestan, R., & Ghaffarzadeh, M. (2024). Soil, air, and water pollution from mining and industrial activities: Sources of pollution, environmental impacts, and prevention and control methods. *Results in Engineering*, 23, 102729. https://doi.org/10.1016/j.rineng.2024.102729

Pjevalica, N., Nikolic, M., & Teslic, N. (2015). *Magnetic Saturation of Permanent Magnet Motor Coil as Key Effect for Initial Rotor Position Detection.* https://www.researchgate.net/publication/282012182_Magnetic_Saturation_of_Permanent_Magnet_Motor_Coil_as_Key_Effect_for_Initial_Rotor_Position_Detection

Popescu, M. (2006). Prediction of the electromagnetic torque in synchronous machines through Maxwell stress harmonic filter (HFT) method. *Electrical Engineering*, 89(2), 117–125. https://doi.org/10.1007/s00202-005-0323-1

Saidur, R. (2010). A review on electrical motors energy use and energy savings. *Renewable and Sustainable Energy Reviews*, 14(3), 877–898. https://doi.org/10.1016/j.rser.2009.10.018

Shin, K.-H., Bang, T.-K., Kim, K.-H., Hong, K., & Choi, J.-Y. (2021). Electromagnetic Analysis and Experimental Study to Optimize Force Characteristics of Permanent Magnet Synchronous Generator for Wave Energy Converter Using Subdomain Method. *Processes*, 9(10), 1825. https://doi.org/10.3390/pr9101825

Tagliaferri, C., Evangelisti, S., Acconcia, F., Domenech, T., Ekins, P., Barletta, D., & Lettieri, P. (2016). Life cycle assessment of future electric and hybrid vehicles: A cradle-to-grave systems engineering approach. *Chemical Engineering Research and Design*, 112, 298–309. https://doi.org/10.1016/j.cherd.2016.07.003

Tong, N., Zhang, C., Li, Y., Chen, Y., Yang, W., Li, J., Yu, P., & Li, K. (2025). Research on temperature rise characteristics of built in permanent magnet synchronous motor coupled with magnetic thermal flow field. *Case Studies in Thermal Engineering*, 75, 107030. https://doi.org/10.1016/j.csite.2025.107030

Zhu, Z. Q., Liang, D., & Liu, K. (2021). Online Parameter Estimation for Permanent Magnet Synchronous Machines: An Overview. *IEEE Access*, 9, 59059–59084. https://doi.org/10.1109/ACCESS.2021.3072959

Data & Code Availability Statement

All original data collected for this study can be found here.

Acknowledgements

The author wants to thank **Dr. Andrea Giusti**, an associate professor in thermofluids at Imperial College London, and **Marcin Kedziera**, a PhD candidate in Artificial Intelligence at the University of Edinburgh. Both advised on how to build an academic paper and provided feedback during the production of the paper.

Author Biography

Guilherme Yuji Oliveira Kikuchi is a high school student at Colégio Miguel de Cervantes, São Paulo, Brazil. He is interested in physics, electrical engineering, and quantum computing, focusing on electromagnetism. He took part in optical engineering classes and quantum mechanics classes at the Brown pre-college summer program in 2025. The motivation behind this work's idea was to understand the effects of magnetic saturation on the efficiency of electric machines, after producing papers for IB physics SL and extended essay. He is currently working on the development of his NGO in the efforts of democratizing access to practical experiments in electrodynamics and electromagnetism for all public-school students in Brazil. In the future, he aspires to pursue a major in electrical engineering with a minor in physics at an American university.

Mentor Contribution Statement

Dr. Andrea Giusti and **Mr Marcin Kedziera** served as mentors during the IRIS Indigo Research Program in winter 2025-26. Their support was grounded in helping the student understand how an academic paper is written and what it consists of. Moreover, they provided constructive feedback on many parts of the writing process in order to improve clarity, accuracy, style, and register. Finally, their role was fundamentally and exclusively advisory, and this statement further acknowledges their contribution while confirming that all research and writing were completed independently by the student author.